

# Cosmology on a gravitational wave background

Tonatiuh Matos<sup>1</sup>,<sup>1</sup>★† Luis A. Escamilla,<sup>2</sup> Maribel Hernández-Marquez<sup>3</sup>★ and J. Alberto Vázquez<sup>2</sup>★

<sup>1</sup>*Departamento de Física, Centro de Investigación y de Estudios Avanzados del IPN, AP 14-740, Ciudad de México 07000, México*

<sup>2</sup>*Instituto de Ciencias Físicas, Universidad Nacional Autónoma de México, Apdo. Postal 48-3, 62251 Cuernavaca, Morelos, México*

<sup>3</sup>*Instituto de Ciencias Nucleares, Universidad Nacional Autónoma de México, Apdo. Postal 70-543, Deleg. Coyoacán, C.P. 04510 CDMX, México*

Accepted 2024 February 12. Received 2024 February 5; in original form 2023 December 28

## ABSTRACT

It is a fact that the universe lives on a gravitational wave background (GWB), which is extra space–time energy that is not contained in Einstein’s field equations. In a previous work, this energy is treated as a property of space–time and not as a source. With this in mind, a new model was developed that incorporates this energy to explain the current accelerated expansion of the universe where the GWB was incorporated by extending Einstein’s equations to  $R_{\mu\nu} - \frac{1}{2}Rg_{\mu\nu} + \frac{2\pi^2}{\lambda^2}g_{\mu\nu} = \kappa^2 T_{\mu\nu}$ , where  $\lambda$  is the Compton wavelength of the cosmological scale graviton. In the present work, we show that this extended form agrees very well with the observations of cosmic chronometers, baryon acoustic oscillations, and Pantheon SN Type Ia, reproducing the observational data with a  $\Delta\chi^2 = 3.26$  in favour of the current model compared to the  $\Lambda$ CDM. The favoured values by these observations are  $\Omega_{0m} = 0.311 \pm 0.065$ ,  $H_0 = 68.3 \pm 1.4 \text{ km s}^{-1} \text{ Mpc}^{-1}$ , and  $\Omega_{0k} = 0.001 \pm 0.011$ . We also find excellent agreement of this model with the cosmic microwave background and the mass power spectrum. We conclude that this model is an excellent alternative to explain the accelerated expansion of the universe without incorporating the cosmological constant or any type of extra matter.

**Key words:** cosmology: dark energy – cosmology: theory.

## 1 INTRODUCTION

In the realm of cosmology, one of the most significant revelations of the past century was the observation that the universe is not only expanding but is also experiencing an accelerated expansion. This extraordinary finding defied our expectations and sparked research endeavours to comprehend the underlying causes driving this peculiar behaviour. It is within this context that the concept of dark energy emerged as a compelling explanation for the accelerated expansion. However, the fundamental nature of dark energy still remains as a perplexing enigma, and unravelling its mysteries continues to be a captivating pursuit. Despite the multitude of proposals and ideas aimed to decipher this phenomenon, we have not yet arrived to a fully convincing solution (see for instance, Frusciante & Perrenon 2020; Bamba 2022; Poulin, Smith & Karwal 2023).

In a previous study (Matos & L-Parrilla 2021b), a novel model dubbed as the Compton Mass Dark Energy (CMaDE) was introduced, whose main goal is to incorporate the gravitational wave background (GWB), and it could be a viable explanation of the accelerated expansion of the universe. Very recently it has been demonstrated by several observatories that the universe is immersed in a GWB (Agazie et al. 2023; Antoniadis et al. 2023; Reardon et al. 2023; Xu et al. 2023), in this case the frequencies observed are of the order of nanohertz and their origin is still unknown. However, there

is no clear justification for restricting the GWB solely to nanohertz frequencies and therefore we will consider their wavelength may be extended to other scales, specifically those at cosmological scales. In this context, we let the specific origin of the GWB for other works, but it is important to clarify that it is an additional energy not incorporated into the Einstein’s equations a priori, which is intrinsically connected to the space–time metric. Thus, similar to the aforementioned study, the proposal is to incorporate the GW energy of space–time into Einstein’s equations. GWs and the mediator of the gravitational interaction, here for simplicity named as graviton, has zero mass. To study the universe, we focus on frequencies at cosmological scales. In Matos & L-Parrilla (2021b; see also Escobar-Aguilar, Matos & Jimenez-Aquino 2023) this energy was introduced into the Einstein’s equation to obtain

$$R^{\mu\nu} - \frac{1}{2}g^{\mu\nu}R + \frac{2\pi^2}{\lambda^2}g^{\mu\nu} = \kappa^2 T^{\mu\nu}, \quad (1)$$

where  $\kappa^2 = 8\pi G/c^4$ ;  $G$  is Newton’s gravitational constant, and  $\lambda$  is the Compton wavelength of the cosmological scale graviton, which at cosmological scales depends only on the time  $t$  coordinate due to the expansion of the universe. The derivation of equation (1) in the reference Matos & L-Parrilla (2021b) may seem controversial, but in the present work, we will only consider the equation (1) from the phenomenological point of view, the results presented here justify this choice. For a similar approach, but with a completely different philosophy, see e.g. Li (2004a); Cai (2007).

In a previous study (Matos & Tellez-Tovar 2022), it was demonstrated that these equations not only provide an explanation for the accelerated expansion of the universe but may also exhibit an agree-

\* E-mail: [tonatiuh.matos@cinvestav.mx](mailto:tonatiuh.matos@cinvestav.mx) (TM);  
[maribel.hernandez@nucleares.unam.mx](mailto:maribel.hernandez@nucleares.unam.mx) (MHM);  
[javazquez@icf.unam.mx](mailto:javazquez@icf.unam.mx) (JAV)

† Part of the Instituto Avanzado de Cosmología (IAC) Collaboration.

ment with key cosmological observations such as the mass power spectrum (MPS) and the cosmic microwave background (CMB) radiation. However, it should be noted that the works mentioned in Matos & L-Parrilla (2021b) and Matos & Tellez-Tovar (2022), were carried out using an approximation where the covariant derivative of the energy–momentum tensor  $T^{\mu\nu}_{;\nu}$  disappeared. Although this approach results in a minimal violation of the general covariance principle, it is important to address this issue. Therefore, in the present study, we aim to remove the approximation and evaluate the performance of the CMADE model against the standard  $\Lambda$ CDM cold dark matter ( $\Lambda$ CDM) model by confronting it with background data.

The main result of this work is the following. We show that if we consider part of the primordial GW produced during the big bang, this causes the accelerated expansion of the Universe, similar to a tsunami that expands in the sea. With this hypothesis we can explain the observations of SN Ia supernovae, baryon acoustic oscillations, and cosmic chronometers (CCs), provided that the current value of the Hubble constant is  $H_0 = 69.9 \text{ km s}^{-1} \text{ Mpc}^{-1}$ , and according to the observations of the CMB by *Planck* and from the MPS let  $H_0 = 68 \text{ km s}^{-1} \text{ Mpc}^{-1}$ . This result gives solid validity to take equation (1) as a good model to explain cosmological observations.

## 2 THE CMADE MODEL

In order to obtain the conservation equations of the system, in a Friedman-Lemaître-Robertson-Walker (FLRW) universe, we perform the covariant derivative of equation (1). Observe that  $G^{\mu\nu}_{;\nu} = 0$  by construction and  $g^{\mu\nu}_{;\nu} = 0$  because the metric is compatible with respect to the connection. For index  $\mu \neq 0$  the covariant derivative of equation (1) is an identity, but for  $\mu = 0$ , we obtain

$$\dot{\mathcal{M}}c^2 = -\kappa^2 (\dot{\rho} + 3H(\rho + p)), \quad (2)$$

where

$$\mathcal{M} = \frac{2\pi^2}{\lambda^2}, \quad (3)$$

is the extra term in the Einstein's equations; where  $H = \dot{a}/a$  is the Hubble parameter and  $\rho$  and  $p$  are the total energy density and pressure of the system, respectively. Here, we consider the components of the universe are the matter  $\rho_m$ , which is made up of dark matter  $\rho_{dm}$  and baryons  $\rho_b$ , and radiation  $\rho_r$  made up of neutrinos  $\rho_\nu$ , and photons  $\rho_\gamma$ . Bearing in mind, we know the equations of state for baryons and radiation, hence  $\dot{\rho}_b + 3H\rho_b = 0$  and  $\dot{\rho}_r + 4H\rho_r = 0$ , then we can plug in these results into equation (2). On the other hand, because the lack of information about the nature of dark matter, as a first approximation, we can assume that it is made up of dust with  $p_{dm} = 0$ , just like baryons. The main difference with the previous works (Matos & L-Parrilla 2021b; Matos & Tellez-Tovar 2022) is that here, we let the dark matter interact with the GWB energy of space–time, avoiding the violation of the general covariance principle. Furthermore, we know that  $\rho = \rho_m + \rho_r = \rho_{dm} + \rho_b + \rho_r$ , and  $p = p_r + p_m = \frac{1}{3}\rho_r$ . Using these results, the equation (2) becomes

$$\begin{aligned} k_c \dot{\mathcal{M}}c^2 &= -\kappa^2 (\dot{\rho}_{dm} + 3H\rho_{dm}), \\ \dot{\rho}_b &= -3H\rho_b, \\ \dot{\rho}_r &= -4H\rho_r, \end{aligned} \quad (4)$$

where  $k_c$  is a bias parameter that mediates the contribution of the space–time energy of the GWB to dark matter.

Next, we derive an equation for  $\mathcal{M}$ . We know that the wavelength  $\lambda$  satisfies the relation  $\lambda = (c/H_0)R_H$  (Matos & L-Parrilla 2021b),

with

$$R_H = H_0 \int \frac{dt}{a} = H_0 \int \frac{e^{-N}}{H} dN. \quad (5)$$

It is convenient to use the e-folding coordinate  $N$  defined as  $N = \ln(a)$ . We denote the derivative with respect to  $t$  with an over dot, and a prime means the derivative with respect to  $N$ . Then, from equation (3) we have that

$$\mathcal{M}' = -\frac{4\pi^2}{\lambda^3} \lambda'. \quad (6)$$

Thus, we use equation (5) to obtain

$$\mathcal{M}' = \pm \frac{\sqrt{2}c}{\pi} \mathcal{M}^{3/2} \frac{e^{-N}}{H}. \quad (7)$$

However, different frequencies of the fluctuations may contribute in a different way to the accelerated expansion, that is part of these fluctuations can be transformed into black holes, structures of the universe, etc. To mediate this contribution, we can set a bias parameter  $Q$  in front of the equation (7). Equation (4) together with the Friedmann equation

$$H^2 + \frac{k}{a^2} - \frac{\mathcal{M}c^2}{3} = \frac{\kappa^2 \rho}{3}, \quad (8)$$

where  $k = 1, -1, 0$  is the curvature parameter, are a complete set of equations for the variables  $\rho_b$ ,  $\rho_r$ ,  $\rho_{dm}$ , and  $\mathcal{M}$ . It is convenient to rewrite these equations in terms of dimensionless quantities, then we introduce

$$\Omega_X^0 = \frac{\rho_X \kappa^2}{3H_0^2} = \Omega_{0X}^0 a^{-3(1+\omega_X)}, \quad (9)$$

for each component of the system and  $\mathcal{H} = H/H_0$ , where the second identity is valid only for barotropic fluids with  $\omega_X = \text{constant}$ . Observe that in the definition of  $\Omega_X^0$ , we use  $H_0$  instead of the traditional  $H$ . Therefore, we obtain a complete system of equations

$$\begin{aligned} \mathcal{H}^2 &= \Omega_b^0 + \Omega_{dm}^0 + \Omega_r^0 + \Omega_{0k}^0 e^{-2N} + \Omega_{\mathcal{M}}^0, \\ \Omega_{dm}^{0'} &= -3\Omega_{dm}^0 - k_c \Omega_{\mathcal{M}}^{0'}, \\ \Omega_b^{0'} &= -3\Omega_b^0, \\ \Omega_r^{0'} &= -4\Omega_r^0, \\ \Omega_{\mathcal{M}}^{0'} &= Q \frac{\sqrt{6}}{\pi} \Omega_{\mathcal{M}}^{3/2} \frac{e^{-N}}{\mathcal{H}}, \end{aligned} \quad (10)$$

where the first one is the Friedmann equation. Observe that due to the  $\pm$  sign of the square root of  $\mathcal{M}$ , we have the possibilities that  $Q$  can be positive or negative in the evolution of  $H$ .

Note that the quantity  $\mathcal{M}$  has no free parameters, instead the CMADE model has two bias parameters,  $Q$  and  $k_c$ . If we compare this model with others, this fact reduces the CMADE model certain competitiveness, but on the other hand, the fact that the CMADE model can give a real answer to the nature of dark energy gives this model great relevance.

## 3 COMPARING WITH COSMOLOGICAL OBSERVATIONS

It is straightforward to find numerical solutions of the system (10); as a test, we use the initial conditions obtained from the  $\Lambda$ CDM model, and implemented a PYTHON code with an Adams–Badsforth–Moulton algorithm that integrates the system from  $N = 0$  to  $N = -17$ . As a proof of the concept, we set as initial conditions  $\mathcal{H}_0 = 1$ ,  $\Omega_{0b}^0 = 0.044$ ,  $\Omega_{0dm}^0 = 0.27$ ,  $\Omega_{0r}^0 = 9.539 \times 10^{-5}$ , and  $\Omega_{0k}^0 = 0.08$

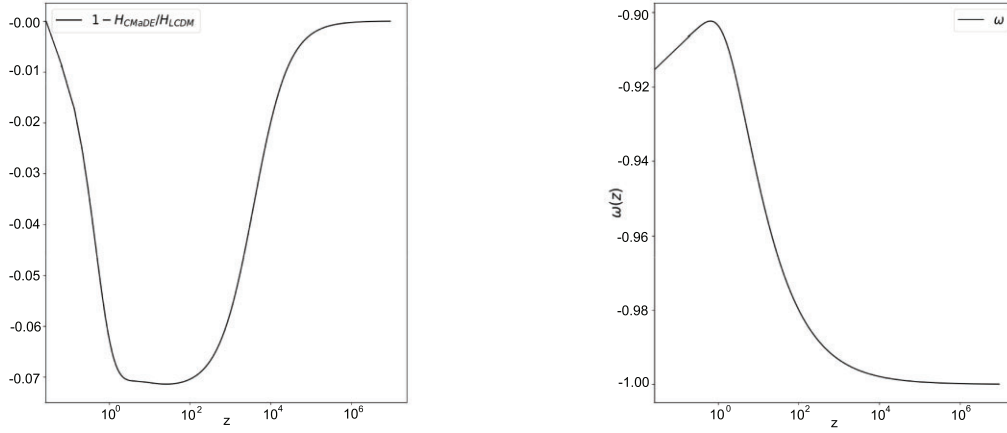


**Figure 1.** In the left panel, we show the relationship of the Hubble parameters  $1 - H_{\text{CMaDE}}/H_{\text{LCDM}}$ , given by the solution of the system of equation (10) and the corresponding one of  $\Lambda$ CDM. We observe a small difference of less than 7 per cent between both functions. Here, we set  $\mathcal{H}_0 = 1$ ,  $\Omega_{\text{ob}}^0 = 0.044$ ,  $\Omega_{\text{dm}}^0 = 0.27$ ,  $\Omega_{\text{or}}^0 = 9.539 \times 10^{-5}$ , and  $\Omega_{\text{ok}}^0 = 0.08$  for both models. In the left panel, we see the evolution of EoS (12). Notice that the effective EoS converges to  $-1$  at high-redshifts, specially at recombination era.

for both the CMaDE and the  $\Lambda$ CDM models. In Fig. 1, we show a comparison of the Hubble parameter behaviour for the CMaDE and  $\Lambda$ CDM models. In the left panel of this figure, we establish the current value of the Hubble constant  $\mathcal{H}_0 = 1$  to compare both evolutions. We plot the rate  $1 - H_{\text{CMaDE}}/H_{\text{LCDM}}$  in order to see the difference between both models and it can be noticed that its difference does increase at small redshifts, within observable regions, but converges to the  $\Lambda$ CDM at the present time as well as at the early universe. We think this could be an indication that the CMaDE model might ameliorate the Hubble constant tension by maintaining consistency with the CMB and modifying mainly the late time observables.

Now, we introduce an effective equation of state (EoS) for the CMaDE model. In order to do so, we define a function  $w_{\text{eff}}$  such that

$$\Omega'_{\mathcal{M}} + 3(1 + w_{\text{eff}})\Omega_{\mathcal{M}}^0 = 0. \quad (11)$$

We use the last equation of system (10) to obtain the effective EoS

$$w_{\text{eff}} = -Q \sqrt{\frac{2}{3}} \sqrt{\Omega_{\mathcal{M}}^0} \frac{e^{-N}}{\pi \mathcal{H}} - 1. \quad (12)$$

We plot the results in the right panel in Fig. 1. Note that the EoS tends to be  $-1$  in the early universe, then changes its value after recombination. We will see that the CMB values are very much in agreement with this behaviour.

Finally, we want to compare the CMaDE model with the main cosmological observations at the background level, and let the perturbative study for future works. In order to do this, we performed a statistical analysis of our model parameter space with a publicly available Bayesian inference code named `SimpleMC` (Aubourg et al. 2015; Slosar & Vazquez Slosar & Vazquez), which includes the `dynesty` library (Speagle 2020), a nested sampling algorithm used to compute the Bayesian evidence. The data sets used in this work consist of:

(i) Baryon acoustic oscillation (BAO) measurements. The BAOs utilized in this study are obtained from Sloan Digital Sky Survey (SDSS), SDSS-II, Baryon Oscillation Spectroscopic Survey (BOSS), and eBOSS. The data sets encompass the SDSS galaxy consensus, quasars, and Lyman  $\alpha$  forests (Beutler et al. 2011; Alam et al. 2017, 2021; Ata et al. 2018; Blomqvist et al. 2019; de Sainte Agathe et al. 2019). The sound horizon is calibrated by using

big bang nucleosynthesis (Aubourg et al. 2015). Henceforth, these measurements will be referred to as BAO.

(ii) The complete catalogue of supernovae from the Pantheon Plus SN Ia sample (referred to as SN). This SN data set builds upon the original Pantheon compilation, aiming to enhance the precision and inclusiveness of the supernova sample. Both the covariance matrix and the data are available in Scolnic et al. (2022).

(iii) The Hubble parameter, denoted as  $H(z)$ , is derived by compiling measurements from CCs, which are old stars functioning as ‘standard clocks’ in cosmology. The CC data set employed in this study is available in the repository <https://gitlab.com/mmoresco/CCcovariance> by M. Moresco.

(iv) We utilize data from the *Planck* satellite to extract information from the CMB. However, our focus solely rests on the cosmological background, excluding perturbations. In this context, the *Planck* data functions as a BAO measurement with a redshift of approximately  $z \approx 1100$ , corresponding to the last dispersion epoch. This implies that we are capturing the angular scale of the sound horizon at a high-redshift. As elaborated in Aubourg et al. (2015), the CMB information on a background level can be condensed into three parameters:  $w_b$  (physical baryon density parameter),  $w_{\text{cb}}$  (physical matter density parameter), and  $D_A(1100)/r_d$ , accompanied by their associated covariance matrix.

Given that we are only focusing on background data the parameters to be used are those relevant to the background only. The flat priors used for these parameters are:  $\Omega_{\text{om}} = [0.1, 0.5]$  for the matter density parameter,  $\Omega_b h^2 = [0.02, 0.025]$  for the baryon density,  $h = [0.4, 0.9]$  for the dimensionless Hubble constant  $h = H_0/100 \text{ km s}^{-1} \text{ Mpc}^{-1}$ , the radiation is negligible so we will set  $\Omega_{\text{or}} = 0$ , and for the curvature’s density parameter  $\Omega_{\text{ok}} = [-0.02, 0.02]$ . For the bias parameters we choose  $k_c = [0, 1]$  and  $Q = [-2, 2]$ .

The results of the parameter inference procedure can be found in Figs 2 and 3: the marginalized posteriors for the parameters; along with Table 1. For best-fitting values (last row of the table), with their  $1\sigma$ , we have:  $\Omega_{\text{om}} = 0.315 \pm 0.053$ ,  $h = 0.699 \pm 0.012$ ,  $\Omega_{\text{ok}} = 0.017 \pm 0.002$ ,  $k_c = 0.83 \pm 0.09$ , and  $Q = -0.67 \pm 0.12$ . To compare how the CMaDE model performs, we assess the fitness to the data via  $-2\Delta \ln \mathcal{L}_{\text{max}} = -2 \ln \mathcal{L}_{\text{max, LCDM}} + 2 \ln \mathcal{L}_{\text{max, CMaDE}}$ , which is the difference between our model’s best-fitting to the data versus  $\Lambda$ CDM’s; and the Bayes’ factor  $B_{1,2} = E_1/E_2$ , or, more specifically, its natural

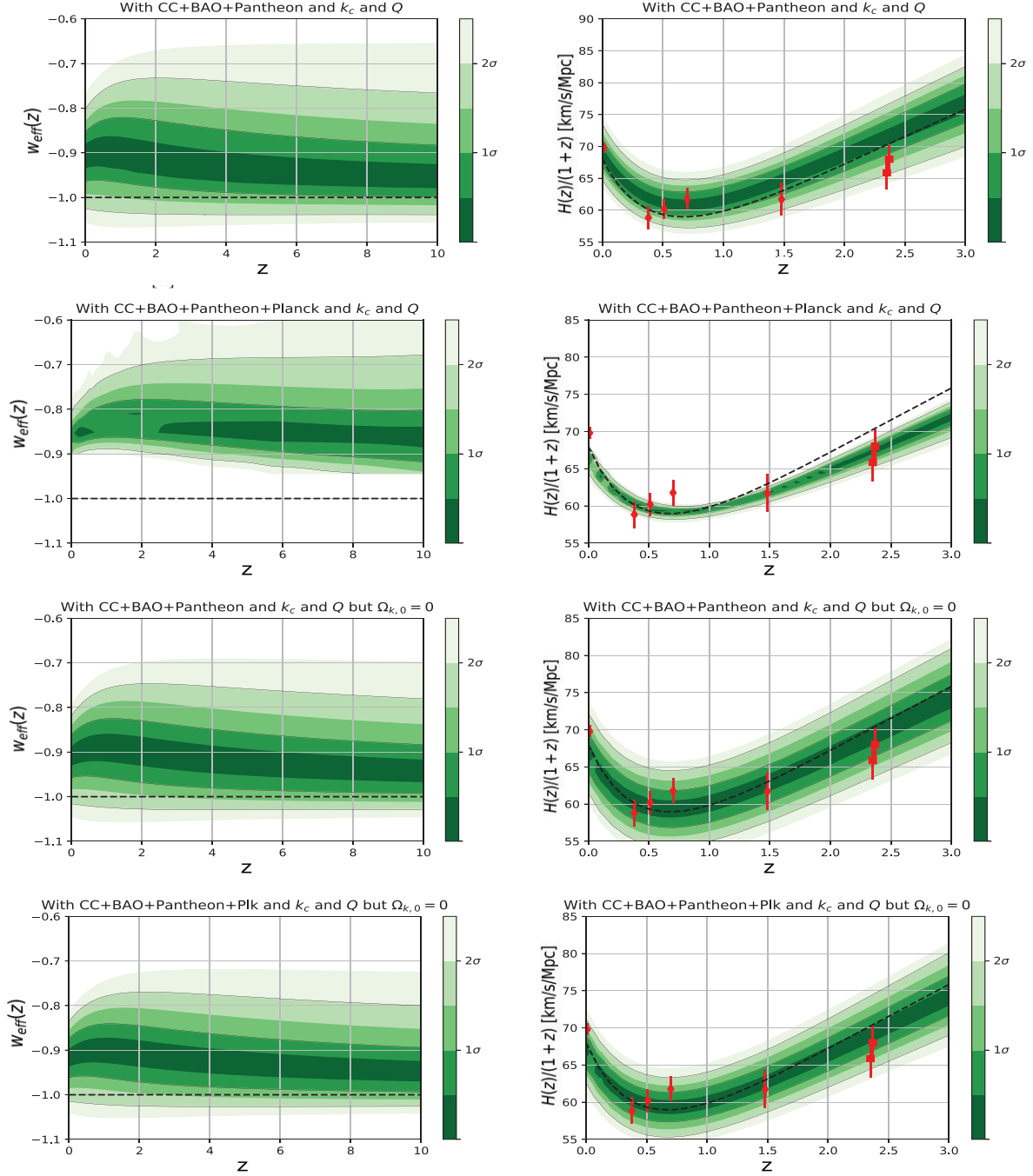


**Figure 2.** Functional posterior probability of the reconstruction with flat curvature. The probability is normalized to each portion of the constant  $z$ , colour-scaled in confidence interval values. The 68 per cent ( $1\sigma$ ) and 95 per cent ( $2\sigma$ ) confidence intervals are represented as black lines. *Left*: the effective EoS (12) and *right*: the Hubble parameter  $H(z)/(1+z)$ . The dashed black line corresponds to the standard  $\Lambda$ CDM values.

logarithm  $\ln B_{1,2}$  where  $E_i$  is the Bayesian evidence for a model  $i$ . In this study, we obtained  $-2\Delta \ln \mathcal{L}_{\text{max}} = 3.65$  in favour of the CMaDE model, indicating a better fitness to the data used. The Bayes' factor obtained is  $\ln B_{1,2} = 2.3$ , indicating that CMaDE is in a slight disadvantage (almost moderate evidence) against the standard model when explaining the observations according to the empirical Jeffrey's scale in Table 2 following the convention from Trotta (2008). This is not unexpected given that our model has two extra parameters and the Bayesian evidence penalizes the added complexity.

On the other hand, in Fig. 2, we observe the functional posteriors for CMaDE's EoS and the Hubble parameter  $H(z)/(1+z)$ . The effective EoS presents quintessence-like behaviour, and as we go further into the past, CMaDE's EoS starts resembling that of  $\Lambda$ CDM as expected. The deviation of CMaDE's Hubble parameter from the standard model is significant enough so that it fits better the BAO data at  $z \approx 2.35$ . We consider this a positive indication for our model since, despite possessing a distinct theoretical foundation and dynamic behaviour in the EoS, our model yields characteristics that

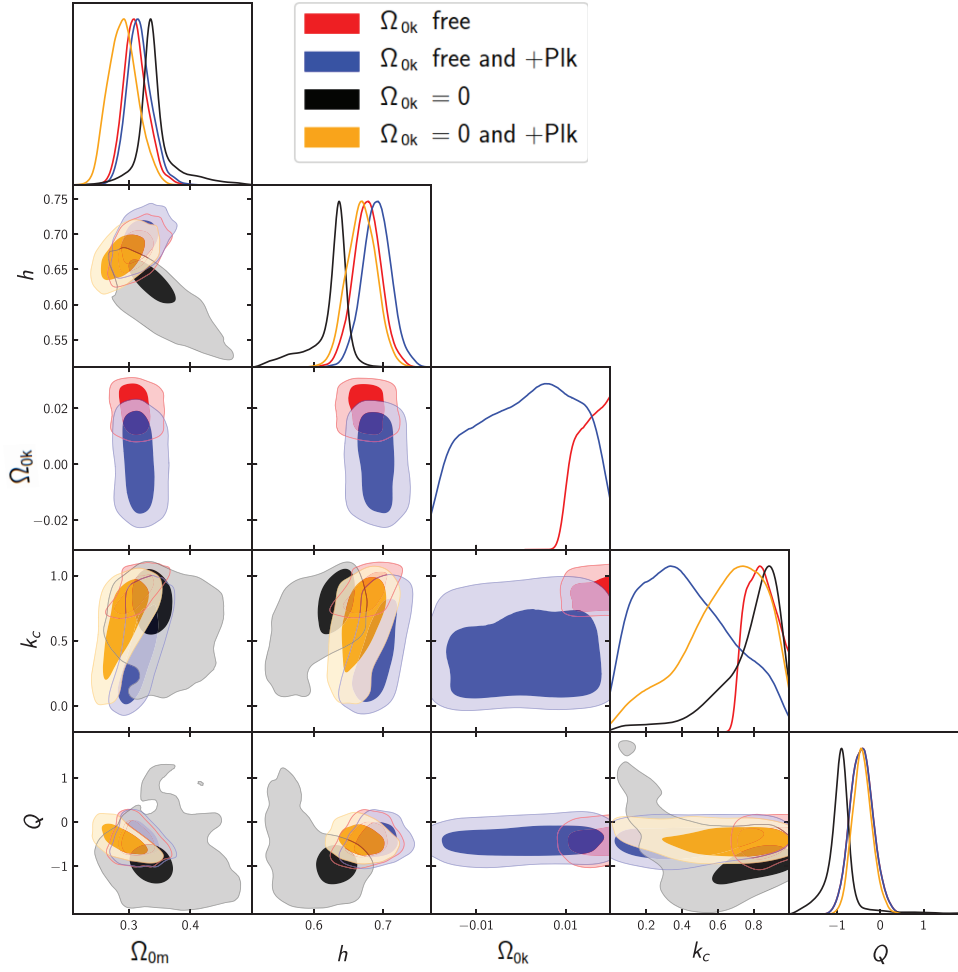


**Figure 3.** Triangular marginal posterior distributions for the inferred parameters; one-dimensional posteriors are displayed over the diagonal and two-dimensional below it; they are colour-coded with the inclusion of curvature and the *Planck* information as shown in the labels.

**Table 1.** Mean values, and standard deviations, for the parameters used throughout the reconstructions. For each model, the last two columns present the Bayes factor, and the  $-2\Delta \ln \mathcal{L}_{\max} \equiv -2 \ln(\mathcal{L}_{\max, \Lambda\text{CDM}}/\mathcal{L}_{\max, i})$  for fitness comparison. Here,  $-2 \ln \mathcal{L}_{\max, \Lambda\text{CDM}} = 1429.71$ ,  $\ln E_{\Lambda\text{CDM}} = -721.59(0.14)$  when not including the *Planck* data set and  $-2 \ln \mathcal{L}_{\max, \Lambda\text{CDM}} = 1431.4$ ,  $\ln E_{\Lambda\text{CDM}} = -726.16(0.14)$  when including it.

Model	$h$	$\Omega_{0m}$	$\Omega_{0k}$	$\ln B_{\Lambda\text{CDM}, i}$	$-2\Delta \ln \mathcal{L}_{\max}$
$\Lambda\text{CDM}$	0.694 (0.016)	0.311 (0.012)	–	0	0
CMADE $\Omega_{0k} = 0$	0.646 (0.029)	0.335 (0.058)	–	0.83 (0.21)	3.21
CMADE	0.683 (0.014)	0.311 (0.065)	0.001 (0.011)	0.10 (0.19)	3.25
With <i>Planck</i> data					
$\Lambda\text{CDM}$	0.682 (0.008)	0.302 (0.011)	–	0	0
CMADE $\Omega_{0k} = 0$	0.685 (0.019)	0.301 (0.051)	–	2.15 (0.21)	1.35
CMADE	0.699 (0.012)	0.315 (0.053)	0.017 (0.002)	2.3 (0.21)	3.65

**Table 2.** Jeffreys’ scale for model selection.

$\ln B_{12}$	Odds	Probability	Strength of evidence
<1.0	<3:1	<0.75	Inconclusive
1.0	~3:1	0.750	Weak evidence
2.5	~12:1	0.923	Moderate evidence
5.0	~150:1	0.993	Strong evidence

closely resembles those of the standard model and even explains better some observations.

For the comparison of the CMADE model with CMB and MPS, we use the CLASS code (Lesgourgues & Tram 2011; Lesgourgues 2011a, b), with the preferred values for  $k_c = 0.42$  and  $Q = -0.43$  and we use an approximation similar to the one in Matos & Tellez-Tovar (2022). With this modification to the code, we generate Fig. 4 whose best-fitting corresponds to  $H_0 = 68 \text{ km s}^{-1} \text{ Mpc}^{-1}$ ,  $\Omega_{0b} = 0.048$ ,



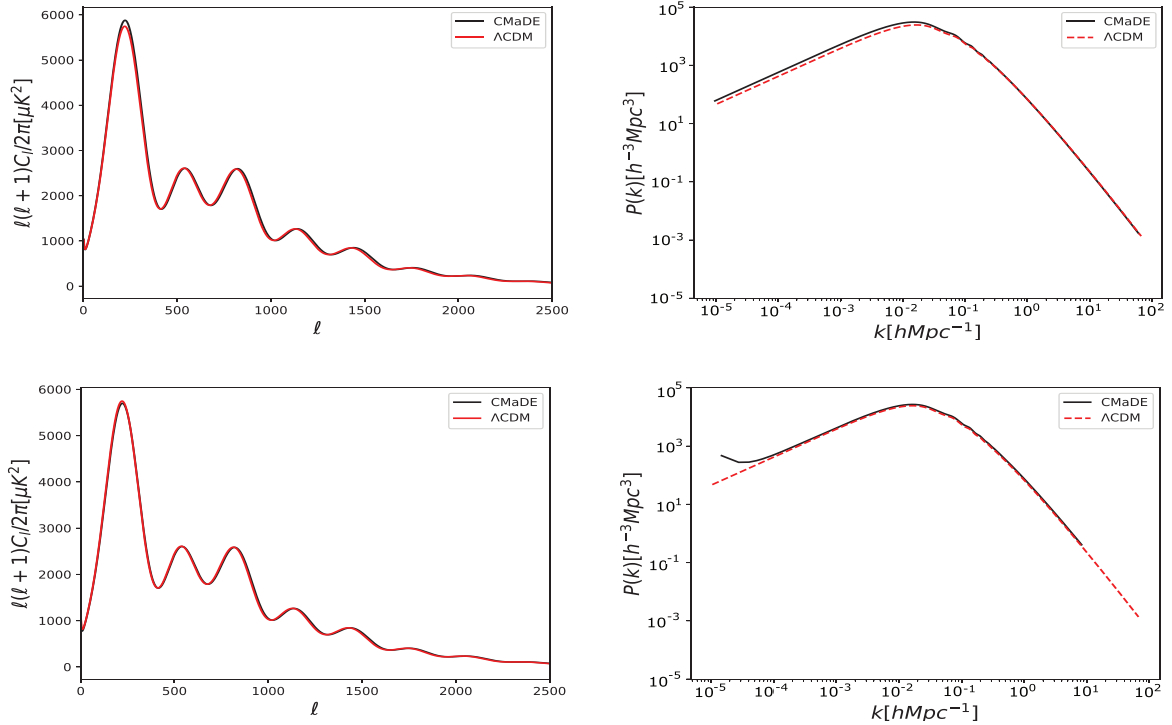


**Figure 4.** In these figures, we only use data from the *Planck* satellite, without local observations, and compare them with the  $\Lambda$ CDM model. *Top:* The CMB and the MPS profiles for the CMADE model. In this figure, we set  $H_0 = 72.6 \text{ km s}^{-1} \text{ Mpc}^{-1}$ ,  $\Omega_{\text{ob}} = 0.044$ , and  $\Omega_{0k} = 0$ . *Bottom:* The CMB and the MPS profiles for the CMADE model. In this figure, we set  $H_0 = 68 \text{ km s}^{-1} \text{ Mpc}^{-1}$ ,  $\Omega_{\text{ob}} = 0.048$ ,  $\Omega_{\text{0dm}} = 0.23$ , and  $\Omega_{0k} = 0.001$ . Note that these last values are very similar to those obtained using only local observations, strongly reducing the  $H_0$  tension.

$\Omega_{\text{0dm}} = 0.23$ , and  $\Omega_{0k} = 0.001$ . We see a very good coincidence with the best-fitting to the CMB and MPS of  $\Lambda$ CDM and consistency with the values of the previous results.

#### 4 CONCLUSIONS

In this work, we follow the idea of Matos & L-Parrilla (2021b) where the energy of space-time fluctuations produced by the big bang is incorporated into Einstein's equations. The novelty of this model is that the GWB energy produced during the big bang is treated as a property of space-time and not as a source, that is this energy appears on the left side of Einstein's equations. With this in mind, Einstein's equation (1) contains an additional term  $\frac{2\pi^2}{\lambda^2}$  that incorporates the energy of these fluctuations in space-time if  $\lambda$  is the Compton wavelength of the cosmological scale graviton. In Matos & L-Parrilla (2021b), it was found that these fluctuations can explain the accelerated expansion of the universe and in Matos & Tellez-Tovar (2022), it was shown that these fluctuations represented in this new term in Einstein's equations are in agreement with the main observations of cosmology profiles of MPS and CMB.

The main differences of this model with those previously published are the following. The first is that the CMADE model may have a strong physical basis, that is that the GWB may be the reason why the universe is expanding with acceleration. This gives us an answer to the nature of dark energy. The second is that the  $\mathcal{M}$  does not have free parameters, the two parameters that appear,  $Q$  and  $k_c$  are bias parameters to measure the amount of energy of the GWB that contributes to the accelerated expansion of the universe,  $k_c$  is the proportion of this energy that contributes to dark matter. But in fact,  $\mathcal{M}$  has no free parameters. Third, this model fits better to closer

observations than the  $\Lambda$ CDM. This fact also implies that the Hubble constant is  $68.3 \text{ km s}^{-1} \text{ Mpc}^{-1}$  when the CMB constraints are not taken into account, and is  $68 \text{ km s}^{-1} \text{ Mpc}^{-1}$  when only the CMB constraints are taken into account, the tension of  $H_0$  is greatly reduced, something that we consider remarkable.

Unlike other models where an interaction between dark matter and dark energy is considered, in the CMADE model this is obtained naturally from theory and is not included by hand (van der Westhuizen & Abebe 2024). Furthermore,  $\mathcal{M}$  is related to the wavelength  $\lambda$  of the gravitational interaction which is limited by the size of the observable Universe (Matos & L-Parrilla (2021b)). It is interesting to note that the density related to  $\mathcal{M}$ ,  $\rho_{\mathcal{M}} = \frac{\mathcal{M}c^2}{\kappa^2} = \frac{2\pi^2 c^2}{\kappa^2 \lambda^2}$  has a similar shape to holographic dark energy (HDE; Wu, Cai & Zhu 2008) and new agegraphic dark energy (NADE; Wei & Cai 2008) but these types of dark energy are obtained from different principles (the holographic principle and the Károlyházy uncertainty relation; Maziashvili 2007) that attempt to unify quantum mechanics and general relativity. In the previous models and in the CMADE model there is a length-scale, however the length-scale in the HDE model is the future event horizon (Li 2004a) of the universe but only in a universe in eternal acceleration does the event horizon exist (Wu et al. 2008). While in the NADE model the length-scale is the conformal time of the Friedmann–Robertson–Walker universe (Wei & Cai 2008) although in this model there is no causality problem, it was found in Kim, Lee & Myung (2008) and Pasqua, Chattopadhyay & Khomenko (2013) that there are instabilities in the model.

Note that the CMADE model does not use an alternative theory of gravity, the only difference of the equation (1) with Einstein's originals is the term  $\frac{2\pi^2}{\lambda^2}$ , which is a consequence of GWB fluctuations in space-time. We can interpret this extra term as the contribution

of the GWB produced by the big bang to the energy of the universe. In the present work, we do not use the approximation  $T^{\mu\nu}_{; \nu} = 0$  to eliminate the small violation of the covariance principle, without this approximation, we show that the agreement between the observations of CC, BAO, and Pantheon is in favour with the CMADE model, with  $\Delta\chi^2 = 3.65$  over  $\Lambda$ CDM. In addition, we compare the CMADE model with the CMB and MPS and we observe that the fit is again in agreement by using the values for the free constants of the model, reducing the so-called tension  $H_0$ . The final conclusion is that the accelerated expansion of the universe can be explained taking into account the GWB energy of space–time, without cosmological constant or modifications of Einstein’s equations.

## ACKNOWLEDGEMENTS

We thank Luis Osvaldo Tellez for his advice and help with the PYTHON codes. This work was partially supported by CONACYT México under grants A1-S-8742, 304001, 376127, and 240512, FORDECYT-PRONACES grant Nos 490769 and I0101/131/07 C-234/07 of the Instituto Avanzado de Cosmología (IAC) collaboration (<http://www.iac.edu.mx/>). JAV acknowledges the support provided by FOSEC SEP-CONACYT Investigación Básica A1-S-21925, UNAM-DGAPA-PAPIIT IN117723 and FORDECYT-PRONACES-CONACYT/304001/2019. LAE acknowledges support from the Consejo Nacional de Humanidades, Ciencias y Tecnologías (CONAHCyT, National Council of Humanities Science and Technology of Mexico) and from the Programa de Apoyo a Proyectos de Investigación e Innovación Tecnológica (PAPIIT) from UNAM IN117723.

## DATA AVAILABILITY

The data underlying this article are available, the data sets encompass the SDSS Galaxy Consensus, quasars, and Lyman  $\alpha$  forests in Alam et al. (2017, 2021), Ata et al. (2018), Beutler et al. (2011), Blomqvist et al. (2019), and de Sainte Agathe et al. (2019).

The SN data set built upon the original Pantheon compilation is available in Scolnic et al. (2022).

## REFERENCES

- Agazie G. et al., 2023, *ApJ*, 951, L8  
 Alam S. et al., 2017, *MNRAS*, 470, 2617  
 Alam S. et al., 2021, *Phys. Rev. D*, 103, 083533  
 Antoniadis J. et al., 2023, *A&A*, 678, 48  
 Ata M. et al., 2018, *MNRAS*, 473, 4773  
 Aubourg E. et al., 2015, *Phys. Rev. D*, 92, 123516  
 Bamba K., 2022, *LHEP*, 2022, 352  
 Beutler F. et al., 2011, *MNRAS*, 416, 3017  
 Blomqvist M. et al., 2019, *A&A*, 629, A86  
 Cai R.-G., 2007, *Phys. Lett. B*, 657, 228  
 de Sainte Agathe V. et al., 2019, *ApJ*, 878, 47  
 Escobar-Aguilar E. S., Matos T., Jimenez-Aquino J. I., 2023, preprint (arXiv:2303.07111)  
 Frusciante N., Perrenon L., 2020, *Phys. Rept.*, 857, 1  
 Kim K. Y., Lee H. W., Myung Y. S., 2008, *Phys. Lett. B*, 660, 118  
 Lesgourgues J., 2011a, preprint (arXiv:1104.2932)  
 Lesgourgues J., 2011b, preprint (arXiv:1104.2934)  
 Lesgourgues J., Tram T., 2011, *JCAP*, 09, 032  
 Li M., 2004a, *Phys. Lett. B*, 603, 1  
 Matos T., L-Parrilla L., 2021b, *Rev. Mex. Fis.*, 67, 040703  
 Matos T., Tellez-Tovar L. O., 2022, *Rev. Mex. Fis.*, 68, 020705  
 Mazishvili M., 2007, *Phys. Lett. B*, 652, 165  
 Pasqua A., Chattopadhyay S., Khomenko I., 2013, *Int. J. Theor. Phys.*, 52, 2496  
 Poulin V., Smith T. L., Karwal T., 2023, *Phys. Dark Universe*, 42, 101348  
 Reardon D. J. et al., 2023, *ApJ*, 951, L6  
 Scolnic D. et al., 2022, *ApJ*, 938, 113  
 Slosar A., Vazquez J. A., <https://github.com/ja-vazquez/SimpleMC>  
 Speagle J. S., 2020, *MNRAS*, 493, 3132  
 Trotta R., 2008, *Contemp. Phys.*, 49, 71  
 van der Westhuizen M. A., Abebe A., 2024, *J. Cosmol. Astropart. Phys.*, 2024, 048  
 Wei H., Cai R.-G., 2008, *Phys. Lett. B*, 660, 113  
 Wu X., Cai R.-G., Zhu Z.-H., 2008, *Phys. Rev. D*, 77, 043502  
 Xu H. et al., 2023, *Res. Astron. Astrophys.*, 23, 075024

This paper has been typeset from a  $\text{\LaTeX}$  file prepared by the author.